JOURNAL OF APPLIED POLYMER SCIENCE VOL. 18, PP. 3109–3126 (1974)

A Radial Cell Model for a Tubular Polymerization Reactor*

L. SCHRENK and J. L. KUESTER,
Arizona State University, Tempe, Arizona 85281

Synopsis

A cell model for the prediction of temperature and concentration gradients in a nonisothermal tubular polymerization reactor at steady state is presented. Both radial and longitudinal gradients are considered. The complete molecular weight distribution is calculated as well as the leading moments of the distribution. The model is easily reduced to predict the performance of a plug-flow tubular reactor, batch reactor, and continuous stirred tank reactor (CSTR). The specific polymerization mechanism application consists of free-radical initiation, propagation, and combination termination.

INTRODUCTION

A large number of papers have appeared in recent years concerning the prediction of reactor performance when a polymerization reaction is involved. Most have been concerned with either a batch reactor or continuous stirred tank reactor (CSTR) at steady state. A consideration of polymerization in a continuous tubular reactor as well as noniosthermal polymerization reactors of any type have been rare.[1,2] Continuous reactors are normally preferred over batch operation from the standpoint of process flexibility and uniform quality. A nonagitated tubular type can be used when slurries are not involved. Nonisothermal operation is the rule rather than the exception with the isothermal case being an ideal limit only for most commercial processes.

The approach to modeling a polymerization reactor usually involves a number of simplifying assumptions due to the enormous complexities involved. The most common assumptions have been the use of moments to characterize the polymer molecular weight distribution and the incorporation of the pseudosteady-state assumption (PSSA) when a termination reaction is involved. The use of moments greatly eases the computational burdens but may be inadequate when attempting to relate polymer properties to the molecular weight distribution. Thus, the complete molecular weight distribution is preferred. The pseudosteady-state assumption states that the rate of change of concentration of all propagating species in a reaction system which includes both initiation and termination may

* Presented in part at the 66th Annual AIChE Meeting, Philadelphia, November 1973.

be assumed to be zero. While again resulting in mathematical simplification, there is some controversy concerning the validity.

The mathematical model for a nonisothermal tubular reactor consists of conservation equations which are usually formulated as differential equations. Due to the highly nonlinear form of these equations, the solution procedure normally involves a finite difference scheme followed by solution of the resulting algebraic equations. A cell model, as an alternate to the differential model for tubular reactors, has been used.[3-5] For this model, it is assumed that the flow process in a single vessel can be described by flow through a series of perfectly mixed cells. For the steady-state system, this method reduces the equation system to a set of algebraic equations equivalent to a particular form of finite difference equations required in a numerical solution for a differential model. The major advantage in the cell model approach is the retention of physical significance in the actual solution equations. Boundary conditions are usually simplified, and reduction of the reactor model to other types is possible.

It is the objective of this paper to present a computationally efficient cell model of a nonisothermal, tubular polymerization reactor at steady state with radial and longitudinal gradients. An addition polymerization mechanism consisting of initiation, propagation, and combination termination will be used as the example. Reductions of the model system to other reactor types will also be illustrated.

THE EQUATION SYSTEM

A schematic representation of the cell model of a tubular reactor is shown in Figure 1. The mathematical model consists of component mass and energy balances for each cell. Assumptions which will be utilized include the following: (1) the reactor is at steady state, (2) the reactor is a cylindrical tube, (3) there is no mass or heat transfer at the inlet or outlet of the reactor through diffusion or conduction, and (4) kinetic and potential energy effects are negligible.

Conservation Equations

A balance for either component mass or energy for cell (j,k) may be written as

$$F_{z,i,j,k-1} + F_{r,i,j-1,k} - F_{z,i,j,k} + F_{r,i,j,k} + R^*_{i,j,k} = 0. \tag{1}$$

The flow terms F include both bulk and diffusion or dispersion effects,

$$F_{z,i,j,k} = G^*_{z,j,k} + J_{z,i,j,k} \tag{2}$$

and

$$F_{r,i,j,k} = G^*_{r,j,k} + J_{r,i,j,k}. \tag{3}$$

For the component mass balance, G^* is equal to the product of the total mass flow rate G and the component mass fraction. For the energy balance,

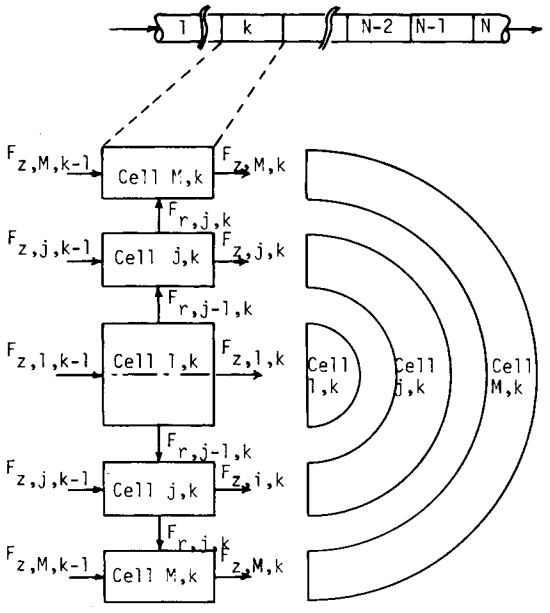

Fig. 1. Representation of the radial diffusion model.

G^* is the product of the total mass flow rate and stream enthalpy H. The dispersion term J is assumed to be proportional to the driving force difference between adjacent cells,

$$J_{z,i,j,k} = \alpha_{z,i,j,k}(X_{i,j,k} - X_{i,j,k+1}) \tag{4}$$

$$J_{r,i,j,k} = \alpha_{r,i,j,k}(X_{i,j,k} - X_{i,j+1,k}), \tag{5}$$

where X is the component mass fraction for the component mass balance and the cell temperature for the energy balance. The source term R^* in eq. (1) is defined for the component mass balance as the rate of appearance of the component,

$$R^*_{i,j,k} = M_i V_{j,k} \sum_l \nu_{i,l} R_{j,k,l} \tag{6}$$

where M_i is the component molecular weight, V is the cell volume, ν is a reaction stochiometric coefficient, and R is the intrinsic rate of reaction. The summation is over all independent reactions. For the energy balance,

$$R^*_{i,j,k} = -V_{j,k} \sum_l R_{j,k,l} \Delta H_{j,k,l} \tag{7}$$

where ΔH is the heat of reaction. Equations (1) through (7) represent the conservation equations necessary to model a tubular reactor at steady state with both axial and radial dispersion effects included. Reductions of this model system for various model types (axial diffusion, radial diffusion, plug flow, batch, CSTR) and boundary conditions are given in Appendix I.

Polymerization Reaction Application

A major fraction of commercial polymers is produced by free-radical polymerization in either bulk or solution. The chemical mechanism for such systems may be described by initiation, propagation, and termination reactions:

$$\mathrm{I} + 2\mathrm{M} \xrightarrow{k_d} 2\mathrm{L}_1 \tag{8}$$

$$\mathrm{L}_n + \mathrm{M} \xrightarrow{k_p} \mathrm{L}_{n+1}, \quad n = 1,2,\ldots,\infty \tag{9}$$

$$\mathrm{L}_n + \mathrm{L}_m \xrightarrow{k_t} \mathrm{D}_{n+m}, \quad n,m = 1,2,\ldots,\infty \tag{10}$$

where I is the initiator, M is the monomer, L is the live polymer, and D is the dead polymer. The rate constants for the propagation and termination steps, k_p and k_t, are assumed to be independent of chain length. Assuming irreversibility, the intrinsic rate equations for each reaction type are as follows:

$$R_i = k_d f[\mathrm{I}] \tag{11}$$

$$R_p = k_p[\mathrm{L}_n][\mathrm{M}] \tag{12}$$

$$R_t = k_t[\mathrm{L}_n][\mathrm{L}_m] \tag{13}$$

where f is an experimentally determined factor describing the efficiency of the reaction, and $[i]$ are the component concentrations.

The reaction scheme represented by eqs. (11) through (13) may now be applied to a specific reactor model represented by eqs. (1) through (7) or a reduction thereof. For any model, the system is represented by an infinite number of coupled nonlinear algebraic equations. The mass fraction values in eqs. (1) through (7) are related to the component concentrations in (11) through (13) by

$$[i]_{j,k} = X_{i,j,k}\left[\frac{\rho_T}{M_i}\right]. \tag{14}$$

Number-average (M_n) and weight average (M_w) molecular weights are obtained from the total polymer concentrations $[\mathrm{P}_n]$ and monomer molecular weight (M_0) as follows:

$$M_n = \frac{\sum_{n=1}^{\infty} n[\mathrm{P}_n]}{\sum_{n=1}^{\infty} [\mathrm{P}_n]} \cdot M_0 \tag{15}$$

$$M_w = \frac{\sum_{n=1}^{\infty} n^2[\mathrm{P}_n]}{\sum_{n=1}^{\infty} n[\mathrm{P}_n]} \cdot M_0. \tag{16}$$

SOLUTION STRATEGY

Solution procedures for the various reactor models will now be presented. The axial diffusion model will not be considered for two reasons: (1) axial diffusion effects are minor for most tubular reactor applications, and (2) it has been shown[4] that a judicious choice of the cell length allows axial dispersion to be accounted for in the cell model.

Radial Diffusion Model Solution

The radial diffusion model requires relations for the effective transport parameters. The relations are as follows.

1. Radial Velocity Profile. The velocity profile is assumed to be constant throughout the reactor with the form dependent on the initial Reynolds number (N_{Re}). For N_{Re} greater than 10^4, the following profile[6] was assumed:

$$v_z = \langle v_z \rangle \left(\frac{5}{4}\right)\left[1 - \left(\frac{r}{R}\right)\right]^{1/7}. \tag{17}$$

For N_{Re} less than 2100, the following laminar, Newtonian profile[6] is assumed:

$$v_z = 2\langle v_z \rangle \left[1 - \left(\frac{r}{R}\right)^2\right]. \tag{18}$$

At intermediate Reynolds numbers, a linear interpolation between the two profiles was assumed to be sufficient.

2. Effective Diffusion Coefficient. For N_{Re} greater than 2100, the mass diffusivity ϵ_m was assumed to be related to the Prandtl mixing length and equal to the eddy diffusivity of mass; for N_{Re} less than 2100, the mass diffusivity was assumed to be equal to the individual molecular diffusivity. The eddy diffusivity of mass is given by Knudsen and Katz[7]:

$$\epsilon_m = (0.4r)^2 \frac{dv_z}{dr}. \tag{19}$$

In order to translate this into an effective diffusivity as defined in Appendix I, the following calculation is made:

$$\gamma_{r,j,k} = \epsilon_{m,j,k}\,(2\pi r_{j,k})\,\Delta Z_{j,k}\,\rho_T \Big/ \left[\left(\frac{r_{j,k} - r_{j-1,k}}{2}\right) + \left(\frac{r_{j+1,k} - r_{j,k}}{2}\right)\right]. \tag{20}$$

3. Effective Conduction Coefficient. For N_{Re} greater than 2100, the conductivity was assumed to be equal to the eddy heat diffusivity; for N_{Re} less than 2100, the conductivity was assumed to be equal to the conductivity of the fluid without mixing. The eddy heat diffusivity as given by Knudsen and Katz[7] is equal to the eddy mass diffusivity. Thus,

$$\epsilon_h = \epsilon_m. \tag{21}$$

The effective conductivity as defined in Appendix I is obtained by

$$\psi_{r,j,k} = C_{pm}\,\gamma_{r,j,k}. \tag{22}$$

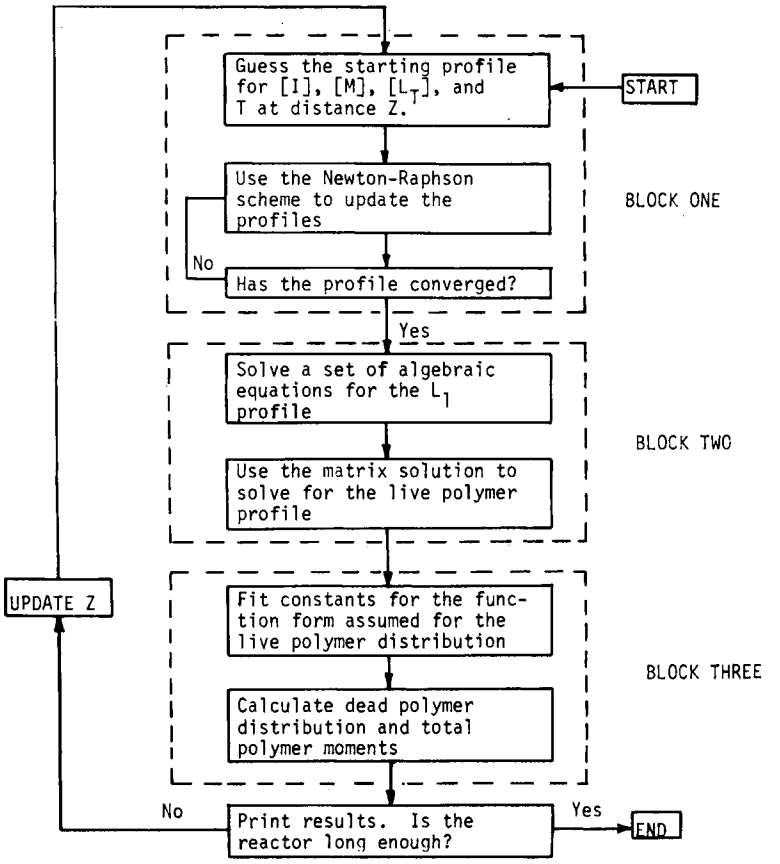

Fig. 2. Procedure for the calculation of radial profiles.

4. Wall Heat Transfer. The heat transferred at the wall of the reactor was assumed to be proportional to a wall heat transfer coefficient and the temperature difference between the fluid in the wall cell and the reactor wall. A constant wall temperature was assumed. The wall heat transfer coefficients were estimated from correlations given in McCabe and Smith.[8]

The solution of the two-dimensional radial model may be broken down into three solution blocks (see Fig. 2). The three blocks will be discussed separately in terms of the necessary inputs to each and the resulting contribution of each block to the overall solution scheme.

The overall solution for a tubular polymerization reactor proceeds by stepping in the axial direction one column of cells at a time (see Fig. 1). The complete profile for all the cells in a column is calculated before moving to the next axial position. The first calculations made at some axial distance Z are those described by Block One. The inputs needed for Block One are the profiles from the preceding column of cells for [I], [M], [L_T], and T. The output will be the final profiles for the column of cells under

consideration. This result requires the simultaneous solution of $4M$ algebraic equations where M is the number of cells in the radial direction. The equations necessary are mass conservation equations for each cell for [M], [I], and [L_T] and an energy balance for each cell. The conservation equations for [M] and [I] and the energy balance are given in Appendix I with the rate terms defined by eqs. (11) through (13). The balance for [L_T] is derived by the summation of the live species equations (L_n) over all n, $n = 1 \rightarrow \infty$. The result for cell j,k is

$$[L_T]_{j,k-1}G_j + [L_T]_{j-1,k}\,\gamma_{L,j-1,k} + [L_T]_{j,k}\,(-G_j - \gamma_{L,j-1,k} - \gamma_{L,j,k} - \rho_T\,V_{j,k}\,k_{t,j,k}\,[L_T]_{j,k}) + [L_T]_{j+1,k}\,\gamma_{L,j,k} + 2\,\rho_T\,V_{j,k}\,k_{d,j,k}\,f_{j,k}\,[I]_{j,k} = 0. \quad (23)$$

Since this set of $4M$ equations is nonlinear, an iterative solution is required. A first-order Newton-Raphson technique was chosen for computational efficiency. If good starting guesses are known, as happens in the reactor marching procedure, then the Newton-Raphson technique will rapidly coverage to the correct answers. This solution procedure can be described by the following steps: (1) Set up Newton-Raphson equations by setting the mass and energy balance expressions equal to functions $f_{i,j,k}$. (2) Use a first-order Taylor series expansion of the functions about estimates of the unknowns in the form

$$f_{i,j,k} = 0 = f_{i,j,k}{}^* + \sum_i \sum_{j=1}^{M} \left[\frac{\partial f_{i,j,k}}{\partial i_{j,k}}\right]^* \Delta i_{j,k} \quad (24)$$

where i may taken on forms of [I], [M], [P_T], and T; and * denotes use of current estimates for evaluation. (3) This expansion results in a set of linear algebraic equations in terms of the error estimates for the unknowns; these may be solved for the error estimates. (4) New estimates may be made for the independent variables. (5) The process (1) through (4) is repeated until the magnitude of the calculated error is less than some preset limit.

The coefficient matrix for the linear equations consists of a band of partial derivatives. Because of the large number of zeros encountered in this matrix, a banded matrix solution procedure employing a Gaussian elimination algorithm was utilized.[9] A forward difference numerical scheme was employed to calculate the matrix of partial derivatives. When the convergence criterion is satisfied, Block Two calculations are commenced.

The Block Two calculations involve the calculation of live polymer, L_n, profiles. The calculation of the concentration profiles for live polymer of chain length one, L_1, is made by a tridiagonal banded matrix solution of equations since the only unknown is the L_1 profile and the equations are linear with respect to L_1. The complete profile could be calculated in a similar manner to that used for L_1; however, this is undesirable because of the huge number of individual components which must be considered. In general, such a technique would require a separate equation set solution of

$4M$ equations for each L_n, where n, the chain length, may be significant for values up to 20,000 for typical polymers. The approach is also undesirable since the $4M$ profiles would have to be saved in order to calculate the profiles for the next set of cells in the axial direction. For these two reasons it was necessary to use another approach for the calculation of the live polymers for chain lengths greater than 1.

It was assumed that the live polymer concentration could be represented by a continuous function of the chain length.[10] This continuous variable approach reduces the infinite number of algebraic equations for each cell involving the live polymer species to one linear ordinary differential equation for each cell with chain length as the independent variable. If $L(n)$ is a continuous function representing the L_n concentration profile, then a first-order Taylor series expansion of $L(n)$ about some chain length n yields

$$\frac{dL(n)}{dn} = \frac{L(n) - L(n - \Delta n)}{\Delta n}. \tag{25}$$

If Δn is chosen to equal 1, then the component mass balance for L_n for column k becomes

$$\rho_T V_j k_{p,j}[M]_j d\frac{L(n)_j}{dn} = \gamma_{L,j-1} L(n)_{j-1} + (-G_j - \gamma_{L,j-1} - \gamma_{L,j} - \rho_T V_j k_{t,j}[L_T]_j) L(n)_j + \gamma_{L,j} L(n)_{j+1} + G_j L^0(n)_j. \tag{26}$$

The equations are a linear set of first-order ordinary differential equations and may be solved by the matrix solution procedure described in Appendix II. The eigenvalues and eigenvectors required for the procedure were found by using a program which employed the method of Rutishauser.[11]

The Block Three calculations, which are dependent on the current live polymer concentration profiles, may now be performed. The function form of $L^0(n)$ must be known to obtain a general solution of the equations. Therefore, an appropriate function form was chosen to characterize the chain length dependence of the concentration profiles. The form obtained for an analytical solution of this reaction mechanism carried out in a CSTR was chosen:

$$L(n)_j = \alpha_j \exp(\beta_j(n - 1)). \tag{27}$$

This form has two arbitrary constants, α_j and β_j. These constants were estimated using a least-squares fit of values of $L(n)$ as a function of n calculated in Block Two. Error estimates from this fit were calculated and the fit was assumed to be adequate. This fit was not only used in the calculation of the next group of $L(n)$ profiles, but also in the calculation of the dead polymer concentration profiles, $[D_n]$.

The dead polymer concentration calculation, see eq. (13), depends on sums of the following form:

$$\sum_{m=1}^{n-1} [L_{n-m}] [L_m]. \tag{28}$$

If these sums were calculated in a direct manner using the results from Block Two, an excessive amount of computer time would be required. Therefore, a modified Euler-Maclaurin summation formula[12] was used:

$$\sum_{m=1}^{n-1} [L_{n-m}]\,[L_m] = \int_1^{n-1} L(n-m)\,L(m)\,dm. \tag{29}$$

Since the form of $L(n)$ is known, the integral in eq. (29) can be easily evaluated and incorporated into the dead polymer calculations. Thus, values of the dead polymer concentrations could be stored at selected chain length intervals. To further reduce the direct calculation of summations required for moment calculations, these dead polymer profiles were also fitted to an equation whose form was assumed by the results of a CSTR solution. The form involved two more constants which were also estimated using a least-squares approach:

$$D(n)_j = \alpha_j' \exp(\beta_j'(n-2))\,(n-1). \tag{30}$$

This result in conjunction with the live polymer result was used to calculate the moments of the total polymer distribution using Euler-Maclaurin summation formula approximations:

$$\lambda_{m,j} = \sum_{n=1}^{\infty} [P_n]_j n^m = \int_1^{\infty} n^m\,(L(n)_j + D(n)_j)\,dn. \tag{31}$$

The final output for each column of cells at a fixed axial position includes the following: (1) values for [I], [M], $[L_T]$, and T; (2) values of the live polymer concentrations; (3) curve-fit parameters which mathematically describe the live polymer profile; (4) values for the dead polymer concentration profile; (5) curve-fit parameters which mathematically describe the dead polymer profile; and (6) moments to describe the polymer molecular weight distribution curves. The axial index is then incremented and the calculations repeated for the desired length of reactor.

Plug-Flow Model Solution

The plug-flow reactor follows the same solution procedure presented for the radial diffusion model using the mass and energy balance equations without diffusion and conduction terms as described in Appendix I. The plug-flow reactor model also assumes a constant velocity profile over the reactor radius. Therefore, the reactor is represented by a set of CSTR's in series in the axial direction. Thus, Block One (Fig. 2) involves the Newton-Raphson solution of four coupled nonlinear algebraic equations. Block Two reduces to the solution of a single linear algebraic equation for $[L_1]$ and the solution of a single linear ordinary differential equation for the remaining live polymer profile; and Block Three reduces to dead and total polymer profile and moment calculations for a single cell.

The relationship of the isothermal batch reactor model to the isothermal plug flow reactor model is as follows:

$$[t]_{\text{batch}} = [Z/(G/\rho_T \pi R^2)]_{\text{plug flow}}. \tag{32}$$

This relationship allows the plug-flow model to predict isothermal batch reactor behavior.

CSTR Model Solution

Further reduction of the radial model to one cell in both the axial and radial directions allows the two-dimensional model to collapse to a CSTR model. The conservation equations thus obtained could be solved in the manner described for the radial model. However, a more versatile and efficient computational technique was employed. The Newton-Raphson scheme of the radial procedure is replaced by the method of Marquardt[13,14] to calculate values of [M], [I], [L_T], and T for the CSTR model. The method of Marquardt has advantages in terms of solution stability. These advantages are discussed by Marquardt.[13] Although the method of Marquardt would be more time consuming than a Newton-Raphson procedure, in general, one would expect the Marquardt procedure to be superior to the Newton-Raphson procedure when poor initial estimates of the unknowns are available, as in a CSTR solution. This nonlinear algebraic equation solution was followed by an analytical calculation of the live and dead polymer distributions. The reduced complexity of the equation system for the CSTR allowed the moments of the total polymer distribution to be calculated by direct summation.

BATCH AND CSTR REACTORS

Tubular polymerization reactor experimental studies reporting molecular weight distributions do not appear to exist in the literature. Hamielec and co-workers[15,16] have polymerized styrene in isothermal batch and CSTR

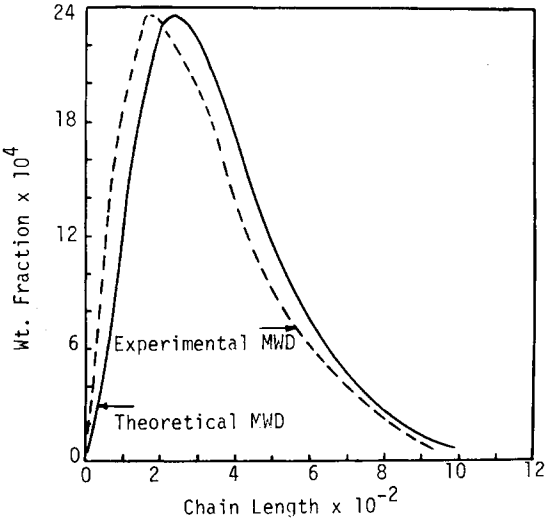

Fig. 3. Molecular weight distribution prediction for a batch reactor. Reactor conditions: $[I]^0 = 0.032$, $[M]^0 = 0.1530$, $T^0 = 348°K$, residence time = 1 hr.

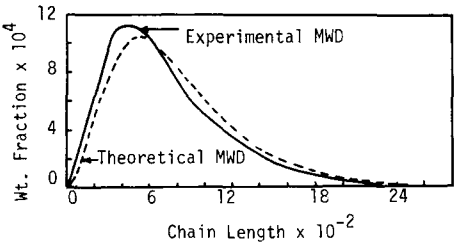

Fig. 4. Molecular weight distribution prediction for a CSTR. Reactor conditions: $[I]^0 = 0.00066$, $[M]^0 = 0.300$, $T^0 = 337°K$, residence time = 2.80 hr.

systems using azobisisobutyronitrile (AIBN) as the initiator and benzene as the solvent and analyzed the product with a gel permeation chromatograph for molecular weight distribution. Thus, to check the performance of the cell model, reductions to the batch and CSTR cases were tested. A description of the reactors and rate constant data are summarized in the original articles. Typical results are shown in Figures 3 and 4. The match appears reasonable, subject to the stated mechanism and assumptions. Improvements might be possible with a consideration of chain transfer reactions and inclusion of the "gel effect" relating initiator efficiency and the termination rate constant to solution viscosity.[17]

TUBULAR REACTOR SIMULATION

The styrene monomer system with AIBN initiator and benzene solvent was again used to test the reactor model for a radial diffusion tubular reactor. Results are shown in Figures 5–8. For the examples illustrated, the heat of propagation and mixture heat capacity were held constant at −29,800 Btu/lb mole and 0.79 Btu/lb mass-°K, respectively. Inlet concentrations were 0.00319 lb moles/ft^3 for the initiator and 0.304 lb/moles/ft^3 for monomer. The radial thickness of the cells was chosen to ensure equal volumes in each cell. In each case, temperature, average degrees of polymerization, and polymer molecular weight divided by repeat unit molecular

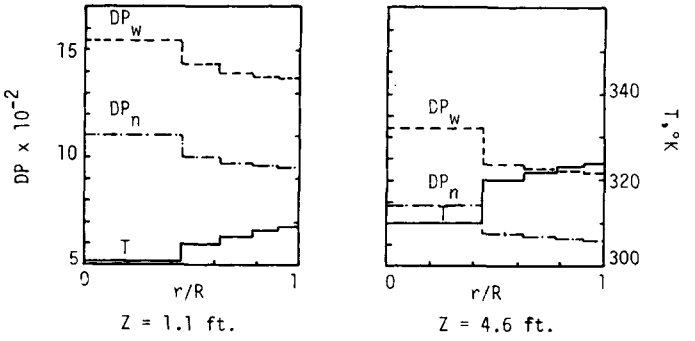

Fig. 5. Radial profiles for a radial diffusion model. Reactor conditions: $R = 0.75$ ft, radial cells = 5, $h_w = 100$, $N_{Re} = 2200$, $\langle v \rangle = 70$, $T^0 = 300°K$, $T_w = 360°K$.

weight (DP_n and DP_w), are shown as a function of radial position at selected reactor lengths. The molecular weight values move in the opposite direction to that of the temperature profiles. The ratio M_w/M_n, often used a an indication of the breadth of the molecular weight distribution, is es-

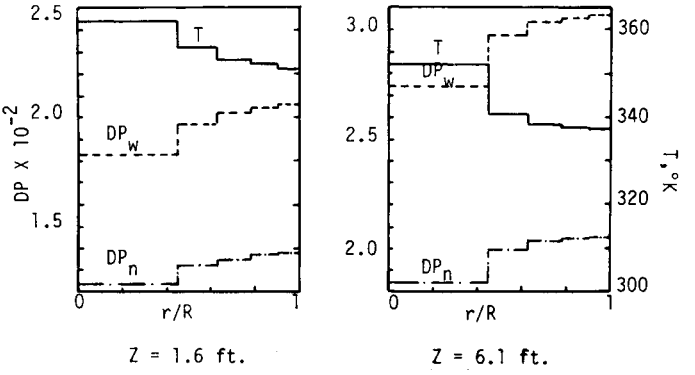

Fig. 6. Radial profiles for a radial diffusion model. Reactor conditions: R = 0.75 ft, radial cells = 5, h_w = 100, N_{Re} = 2200, $\langle v \rangle$ = 70, T^0 = 360°K, T_w = 300°K.

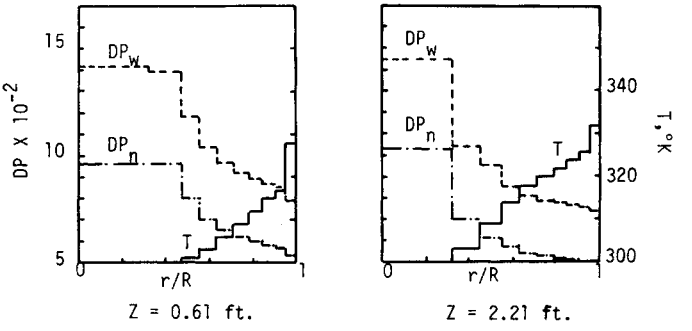

Fig. 7. Radial profiles for a radial diffusion model. Reactor conditions: R = 0.25 ft, radial cells = 10, h_w = 150, N_{Re} = 1330, $\langle v \rangle$ = 100, T^0 = 300°K, T_w = 338°K.

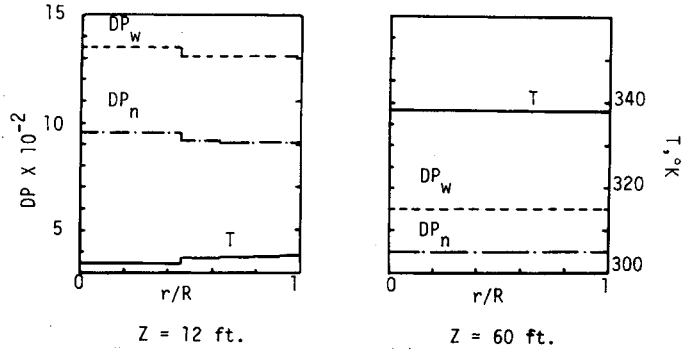

Fig. 8. Radial profiles for a radial diffusion model. Reactor conditions: R = 0.75 ft, radial cells = 5, h_w = 100, N_{Re} = 3700, $\langle v \rangle$ = 120, T^0 = 300°K, T_w = 338°K.

sentially constant (~1.5). Inclusion of viscosity effects (important at high conversions) and/or chain transfer reactions would be required to alter this response. All examples show appreciable radial profiles except Figure 8 where the advanced distance down the reactor has flattened the profiles.

COMPUTATIONAL EXPERIENCE

Computational time requirements were dependent on the particular reactor model and conditions under study. Typical runs using the batch-plug flow and CSTR models (Figs. 3 and 4) could be accomplished in less than 20 sec execution time on the UNIVAC 1110 and CDC 6400 computers. Execution times for the radial gradient tubular model runs varied from about 20 sec for a "mild" condition run (e.g., Fig. 8) to several minutes for more severe conditions.

The effect of transport and kinetic parameters, operating conditions, and solution parameters (cell sizes, numerical convergence limits, etc.) on predicted results were explored with the various models. A complete discussion is beyond the scope of this presentation. With regard to solution parameters, the axial cell dimension for the radial gradient tubular model was the most critical. Thus, for conditions resulting in severe profiles, a larger number of cells (and thus increased computational time) in the axial direction were required to achieve numerical stability. The computational procedure was less sensitive to the cell geometry in the radial direction.

CONCLUSIONS

A computationally efficient model and solution procedure have been presented to tackle the formidable task of solving a polymerization reactor system represented by an infinite system of nonlinear partial differential equations for the radial diffusion continuous model. Reductions to other reactor systems (batch, CSTR, tubular plug flow) is easily accomplished. Extensions of the model to other polymerization reaction systems should be possible.

Appendix I

Reactor Model Summary

This appendix includes a summary of the conservation equations derived in the Equation System section as applied to the following reactor models: (A) CSTR, (B) tubular axial diffusion, (C) tubular radial diffusion, (D) tubular plug flow, and (E) batch.

A. CSTR

1. *Component Mass Balance*

$$GX_i^0 - GX_i + M_i \sum_l \nu_{i,l} R_l V = 0 \tag{AI-1}$$

2. *Energy Balance*

$$GC_{pm}T^0 - GC_{pm}T - V \sum_l R_l \Delta H_l + \text{wall effects} = 0. \tag{AI-2}$$

B. AXIAL DIFFUSION TUBULAR REACTOR (Assume C_{pm} is constant)

1. *Component Mass Balances*

a. Initial Cell

$$GX_i^0 + X_{i,1}(-G - \gamma_{i,1}) + X_{i,2}\gamma_{i,1} + M_i \sum_l \nu_{i,l} R_{1,l} V_1 = 0. \quad \text{(AI-3)}$$

b. General Cell

$$X_{i,k-1}(G + \gamma_{i,k-1}) + X_{i,k}(-G - \gamma_{i,k-1} - \gamma_{i,k}) + X_{i,k+1}\gamma_{i,k} + M_i \sum_l \nu_{i,l} R_{k,l} V_k = 0. \quad \text{(AI-4)}$$

c. Last Cell (cell N)

$$X_{i,N-1}(G + \gamma_{i,N-1}) + X_{i,N}(-G - \gamma_{i,N-1}) + M_i \sum_l \nu_{i,l} R_{N,l} V_N = 0. \quad \text{(AI-5)}$$

2. *Energy Balances*

a. Initial Cell

$$T^0 G\, C_{pm} + T_1(-G\, C_{pm} - \psi_1) + T_2\psi_1 - V_1 \sum_l R_{1,l}\Delta H_{1,l} + \text{wall effects} = 0. \quad \text{(AI-6)}$$

b. General Cell

$$T_{k-1}(G\, C_{pm} + \psi_{k-1}) + T_k(-G\, C_{pm} - \psi_{k-1} - \psi_k) + T_{k+1}\psi_k - V_k \sum_l R_{k,l}\Delta H_{k,l} + \text{wall effects} = 0. \quad \text{(AI-7)}$$

c. Last Cell (cell N)

$$T_{N-1}(G\, C_{pm} + \psi_{N-1}) + T_N(-G\, C_{pm} - \psi_{N-1}) - V_N \sum_l R_{N,l}\Delta H_{N,l} + \text{wall effects} = 0. \quad \text{(AI-8)}$$

C. RADIAL DIFFUSION TUBULAR REACTOR (Assume no bulk flow in the radial direction)

1. *Component Mass Balances*

a. Wall Cell (cell M)

$$X_{i,M,k-1}G_{M,k-1} + X_{i,M-1,k}\gamma_{i,M-1,k} + X_{i,M,k}(-G_{M,k} - \gamma_{i,M-1,k}) + M_i \sum_l \nu_{i,l} R_{M,k,l} V_{M,k} = 0. \quad \text{(AI-9)}$$

b. General Cell

$$X_{i,j,k-1}G_{j,k-1} + X_{i,j-1,k}\gamma_{i,j-1,k} + X_{i,j,k}(-G_{j,k} - \gamma_{i,j-1,k} - \gamma_{i,j,k}) + X_{i,j+1,k}\gamma_{i,j,k} + M_i \sum_l \nu_{i,l} R_{j,k,l} V_{j,k} = 0. \quad \text{(AI-10)}$$

c. Center Cell

$$X_{i,1,k-1}G_{1,k-1} + X_{i,1,k}(-G_{1,k} - \gamma_{i,1,k}) + X_{i,2,k}\gamma_{i,1,k} + M_i \sum_l \nu_{i,l} R_{1,k,l} V_{1,k} = 0. \quad \text{(AI-11)}$$

2. *Energy Balances* (assume C_{pm} is constant and $G_k = G_{k-1}$)

a. Wall Cell (cell M)

$$T_{M,k-1}G_M\, C_{pm} + T_{M-1,k}\psi_{M-1,k} + T_{M,k}(-G_M\, C_{pm} - \psi_{M-1,k}) + \text{wall effects} - V_{M,k} \sum_l R_{M,k,l}\Delta H_{M,k} = 0. \quad \text{(AI-12)}$$

b. General Cell

$$T_{j,k-1}\,G_j\,C_{pm} + T_{j-1,k}\psi_{j-1,k} + T_{j,k}(-G_j\,C_{pm} - \psi_{j-1,k} - \psi_{j,k}) + T_{j+1,k}\psi_{j,k} - V_{j,k}\sum_l R_{j,k,l}\Delta H_{j,k} = 0. \quad \text{(AI-13)}$$

c. Center Cell

$$T_{1,k-1}\,G_1\,C_{pm} + T_{1,k}(-G_1\,C_{pm} - \psi_{1,k}) + T_{2,k}\psi_{1,k} - V_{1,k}\sum_l R_{1,k,l}\Delta H_{1,k} = 0. \quad \text{(AI-14)}$$

D. PLUG FLOW REACTOR

1. *Component Mass Balance*

$$X_{i,k-1}G + X_{i,k}(-G) + M_i\sum_l \nu_{i,l}R_{k,l}V_k = 0. \quad \text{(AI-15)}$$

2. *Energy Balance* (Assume C_{pm} is constant)

$$T_{k-1}\,G\,C_{pm} + T_k(-G\,C_{pm}) - V_k\sum_l R_{k,l}\Delta H_k + \text{wall effects} = 0. \quad \text{(AI-16)}$$

E. BATCH (Assume isothermal)

Same as plug-flow component mass balance using the following independent variable translation:

$$[t]_{\text{batch}} = [Z\,\rho_T\,\pi R^2/G] \text{ plug flow.}$$

Appendix II

Matrix Solution Equations

The continuous variable assumption transforms the M infinite sets of coupled algebraic equations for M coupled cells to a set of M first-order, linear, nonhomogeneous, ordinary differential equations of the following form:

$$\frac{d\,\mathrm{L}(n)_j}{dn} = C_{1,j}\mathrm{L}(n)_{j-1} + C_{2,j}\mathrm{L}(n)_j + C_{3,j}\mathrm{L}(n)_{j+1} + f_j(n) \quad \text{(AII-1)}$$

where the j subscript refers to the cell number in the radial direction.

If the system is put into matrix form, the result is

$$L'(n) = CL\,(n) + F(n) \quad \text{(AII-2)}$$

where

$$L'(n) = \begin{bmatrix} L'(n)_1 \\ L'(n)_2 \\ L'(n)_3 \\ \cdot \\ \cdot \\ \cdot \\ L'(n)_M \end{bmatrix}, \text{ an } M \times 1 \text{ matrix} \quad \text{(AII-3)}$$

$$L(n) = \begin{bmatrix} L(n)_1 \\ L(n)_2 \\ L(n)_3 \\ \cdot \\ \cdot \\ \cdot \\ L(n)_M \end{bmatrix}, \text{ an } M \times 1 \text{ matrix} \quad \text{(AII-4)}$$

$$C = \begin{bmatrix} C_{2,1} & C_{3,1} & 0 & 0 & 0 & 0 & \cdot & 0 \\ C_{1,2} & C_{2,2} & C_{3,2} & 0 & 0 & 0 & \cdot & \cdot \\ 0 & C_{1,3} & C_{2,3} & C_{3,3} & 0 & 0 & \cdot & \cdot \\ 0 & 0 & C_{1,4} & C_{2,4} & C_{3,4} & 0 & \cdot & \cdot \\ \cdot & \cdot & \cdot & \cdot & \cdot & \cdot & \cdot & \cdot \\ \cdot & \cdot & \cdot & \cdot & \cdot & \cdot & \cdot & \cdot \\ \cdot & \cdot & \cdot & \cdot & \cdot & C_{1,M-1} & C_{2,M-1} & C_{3,M-1} \\ 0 & \cdot & \cdot & \cdot & \cdot & 0 & C_{1,M} & C_{2,M} \end{bmatrix} . \quad \text{(AII-5)}$$

an $M \times M$ matrix; and

$$F(n) = \begin{bmatrix} \alpha_1 e^{\beta_1(n-1)} \\ \alpha_2 e^{\beta_2(n-1)} \\ \alpha_3 e^{\beta_3(n-1)} \\ \cdot \\ \cdot \\ \cdot \\ \alpha_M e^{\beta_M(n-1)} \end{bmatrix}, \text{ an } M \times 1 \text{ matrix.} \quad \text{(AII-6)}$$

The form of $F(n)$ is dictated by the particular form assumed for the live polymer distribution in the cell.

The solution to eq. (AII-2) can be obtained as follows[18]:

$$L(n) = Ke^{\Lambda(n-1)}K^{-1}L(1) + Ke^{\Lambda n}\left[\int_1^n e^{-\Lambda n}K^{-1}F(n)\,dn\right] \quad \text{(AII-7)}$$

where Λ and K are matrices of the eigenvalues and eigenvectors of the C matrix. This form of the solution is particularly useful. If the form $F(n)$ is known, the integral may in general be easily disposed of by a term by term integration.

Notation

C_{pm}	mean heat capacity of the reacting mixture (Btu/lb mass-°K)
D_n	dead polymer of chain length n
$D(n)$	continuous function of the dead polymer concentration distribution (lb moles/ft^3)
$[D_n]$	concentration of dead polymer of chain length n (lb moles/ft^3)
DP_n	number average degree of polymerization
DP_w	weight average degree of polymerization
$F_{i,j,k}$	flow rate of component i in lb mass/hr or energy flow rate in Btu/hr out of cell j, k
f	efficiency factor for the initiation reaction
$f_{i,j,k}$	Newton-Raphson function
$G_{j,k}$	total mass flow rate (lb mass/hr) out of cell j,k; also bulk flow in generalized conservation equation
$H_{j,k}$	enthalpy in cell j,k (Btu/lb mass)
$\Delta H_{j,k,l}$	heat of reaction l in cell j,k (Btu/lb mole)
h_w	wall heat transfer coefficient (Btu/ft^2-hr-°K)
I	denotes initiator
$[i]$	denotes concentration of component i in lb moles i/ft^3
Δi	used in the Newton-Raphson procedure to denote the difference between current values of i, i^*, and predicted values of i; $\Delta i = i^* - i$

$J_{i,j,k}$ dispersion term for component mass and energy flow out of cell j,k
k reaction rate constant
L_n live polymer of chain length n
$L(n)$ continuous function of the live polymer concentration distribution (lb moles/ft^3)
$[L_n]$ concentration in lb moles/ft^3 of live polymer of chain length n
$[L_T]$ total live polymer concentration $\sum_{n=1}^{\infty} [L_n]$ (lb moles/ft^3)
M denotes monomer
M_i molecular weight of component i
M_n number-average molecular weight
M_w weight-average molecular weight
N_{Re} Reynolds number
n number of monomer units in the chain length
$[P_n]$ total polymer concentration of chain length n (lb moles/ft^3) = $[L_n] + [D_n]$
R inside reactor radius (ft)
$R_{j,k,l}$ rate of reaction l in cell j,k (lb moles/hr-ft^3); also designates source term in generalized conservation equation
r radial distance (ft)
$T_{j,k}$ temperature of cell j,k (°K)
t time in hours
$V_{j,k}$ volume of cell j,k (ft^3)
v velocity (ft/hr)
$\langle v \rangle$ average tube velocity (ft/hr)
$X_{i,j,k}$ mass fraction of component i in cell j, k; also designates dependent variable in generalized conservation equation
Z axial distance (ft)

Greek Letters

$\alpha_{i,j,k}$ dispersion coefficient in generalized conservation equation
$\alpha,\alpha',\beta,\beta'$ curve fit constants
$\gamma_{i,j,k}$ effective mass diffusion coefficient of component i out of cell j,k (lb mass/hr)
ϵ_m mass diffusivity (ft^2/hr)
ϵ_h heat conductivity (ft^2/hr)
λ_m mth polymer moment about the origin
$\nu_{i,l}$ stoichiometric coefficient of component i in reaction l
$\psi_{j,k}$ effective heat conduction coefficient for heat transfer from cell j,k (Btu/hr-°K)
ρ_T fluid density (lb/ft^3)

Subscripts

d refers to initiation reaction
i refers to a component
j refers to the radial cell number

k refers to the axial cell number
l refers to a reaction
n refers to the number of monomer units in a polymer chain
p refers to the propagation reaction
r refers to the radial direction
w refers to reactor wall
z refers to the axial direction

Superscripts

* indicates evaluation of the expression at the current Newton-Raphson value; also designates source term and bulk flow terms in generalized conservation equation
^{0} indicates an initial or inlet condition for a reactor

The authors acknowledge financial support from the National Science Foundation and Arizona State University Grants Committee.

References

1. R. Cintron, R. Mostello, and J. Biesenberger, *Can. J. Chem. Eng.*, **46**, 434 (1968).
2. S. Lynn and J. Huff, *A.I.Ch.E. J.*, **17**, 475 (1971).
3. H. Deans and L. Lapidus, *A.I.Ch.E. J.*, **6**, 656 (1960).
4. J. L. Kuester and L. Durbin, Paper 27d, 63rd Annual A.I.Ch.E. Meeting, Chicago (1970).
5. J. S. Shastry, L. T. Fan, and L. E. Erickson, *J. Appl. Polym. Sci.*, **17**, 1339 (1973).
6. R. Bird, W. Stewart, and E. Lightfoot, *Transport Phenomena*, Wiley, New York, 1960.
7. J. Knudsen and D. Katz, *Fluid Dynamics and Heat Transfer*, McGraw-Hill, New York, 1958.
8. W. L. McCabe and J. Smith, *Unit Operations of Chemical Engineering*, McGraw-Hill, New York, 1967.
9. *Subroutine GELB*, IBM System/360 Scientific Subroutine Package Version III, IBM Corporation, 1968.
10. R. Zeman and N. R. Amunson, *A.I.Ch.E.J.*, **9**, 297 (1963).
11. B. Carnahan, H. A. Luther, and J. Wilkes, *Applied Numerical Methods*, Wiley, New York, 1969.
12. M. Spiegel, *Mathematical Handbook of Formulas and Tables*, McGraw-Hill, New York, 1968.
13. D. W. Marquardt, *J. S.I.A.M.*, **11**, 431 (1963).
14. J. L. Kuester and J. H. Mize, *Optimization Techniques with Fortran*, McGraw-Hill, New York, 1973.
15. J. H. Duerksen, A. E. Hamielec, and J. W. Hodgins, *A.I.Ch.E.J.*, **13**, 1081 (1967).
16. A. E. Hamielec, J. W. Hodgins, and K. Tebbens, *A.I.Ch.E.J.*, **13**, 1087 (1967).
17. A. W. Hui and A. E. Hamielec, *Ind. Eng. Chem., Process Des. Develop.*, **8**, 105 (1969).
18. N. R. Amundson, *Mathematical Methods in Chemical Engineering: Matrices and Their Application*, Prentice-Hall, Englewood Cliffs, N. J., 1966.

Received January 21, 1974
Revised April 15, 1974